Biophysical Chemistry 40 (1991) 117–125
Elsevier Science Publishers B.V., Amsterdam

BIOCHE 01560

Construction and evaluation of a frequency-domain epifluorescence microscope for lifetime and anisotropy decay measurements in subcellular domains

A.S. Verkman *, Michael Armijo and Kiyohide Fushimi

Departments of Medicine and Physiology, Cardiovascular Research Institute, University of California, San Francisco, CA 94143-0532, U.S.A.

Received 19 July 1990
Revised manuscript received 13 November 1990
Accepted 15 November 1990

Fluorescence lifetime; Epifluorescence microscopy; Fibroblast; Anisotropy decay; Fluorescein; Phase modulation

The measurement of time-resolved fluorescence parameters in living cells provides a powerful approach to study cell structure and dynamics. An epifluorescence microscope was constructed to resolve multi-component fluorescence lifetimes and complex anisotropy decay rapidly in labile biological samples. The excitation source consisted of focused, polarized laser light modulated by an impulse-driven Pockels' cell; parallel acquisition of phase angles and modulation amplitudes at more than 40 frequencies (5–250 MHz) was obtained by multi-harmonic cross-correlation detection. Lifetime decay was measured against standard solutions introduced into the light path proximal to the microscope objective. Anisotropy decay was measured by rotation of a Glan-Thompson polarizer in the emission path. Phase reference light was split from the beam proximal to the microscope. Optical components were selected to avoid depolarization and to optimize fluorescence detection efficiency. The dichroic was replaced by a 1 mm square mirror. Fitting routine statistics were optimized for model discrimination in realistic biological samples. Instrument performance was evaluated using fluorescein in H_2O/glycerol and H_2O/ethylene glycol mixtures and in Swiss 3T3 fibroblasts in monolayer culture. Objective depolarization effects were evaluated by measurement of anisotropy decay using objectives of different numerical aperture. Lifetime and anisotropy decay measured by microscopy (0.5 μm laser spot) agreed with data obtained by cuvette fluorimetry. New biological applications for time-resolved fluorescence microscopy are discussed.

1. Introduction

There has been rapid advancement in the technology for detection of time-resolved fluorescence decay by pulsed laser excitation and parallel detection methods [1–4]. For applications to cytoplasmic and membrane dynamics in living cells, it is necessary to measure complex lifetime and anisotropy decay of fluorophores in regions of single cells. One approach is the development of sensitive array detectors (cameras) for pixel-by-pixel measurement of time-resolved fluorescence with high spatial resolution. However, the sensitivity and ability to resolve multi-component decay in frequency-domain cameras [1,3] and streak cameras [4] is improving but is not at present adequate for single-cell studies.

There are a number of special considerations for microscopy measurements of multi-component fluorescence decay in living cells. To minimize phototoxicity, the measurement should be rapid ($\ll$ 1 min) with high detection efficiency. Reference solutions for lifetime determination must be introduced without movement of the cell sample or objective focus. There should be no depolarization of excitation or emission light by microscope

* To whom correspondence should be addressed at 1065 Health Sciences East Tower.

0301-4622/91/$03.50

components including the dichroic mirror and objective. Because of the non-zero background signal due to instrument and cell autofluorescence, it must be possible to subtract background from sample signal. Excitation wavelength should be adjustable in the range 350–550 nm and modulation frequencies (in frequency-domain measurements) should be in the range < 10 to > 200 MHz to include the majority of biologically useful fluorophores. The spatial resolution should be below 5% of cell dimensions (cell diameters generally 10–30 μm) to permit evaluation of subcellular heterogeneity in time-resolved fluorescence parameters.

We report here the development of optics and analysis methods for the rapid measurement of time-resolved fluorescence parameters by epifluorescence microscopy with submicron spatial resolution. Frequency- and time-domain information was obtained by a multi-harmonic Fourier transform spectrometer described recently [2]. Instrument optics, measurement procedures and analysis software were optimized for studies in biological samples. Instrument performance was evaluated in bulk solutions and living cells by comparison with results obtained by cuvette fluorimetry.

2. Methods

Laser grade fluorescein, 6-carboxyfluorescein (6CF) and 2,7-biscarboxyethyl-5 [and 6]-carboxyfluorescein (BCECF) were obtained from Molecular Probes (Junction City, OR). Swiss 3T3 fibroblasts (ATCC CCL 92) were obtained from the cell culture facility at U.C.S.F. and used between passages 61 and 70. Cells were grown on 18 mm round, 0.12 mm thick glass coverslips at 37 °C in 5% CO_2/95% air in Dulbecco's modified Eagle's medium supplemented with 10% fetal bovine serum.

Cells were loaded with 6CF by a 3 min incubation with 1 mM 6CF in Hank's balanced salt solution (HBSS) at pH 6. Extracellular 6CF was washed with HBSS at pH 7.4. Cells were mounted in a perfusion chamber in which the cell-free surface of the glass coverslip made contact with immersion microscope objectives [5]. The microscope measurement system is described below.

3. Instrument design

3.1. Optics

Fig. 1 shows a schematic diagram of the time-resolved epifluorescence microscope system. Fig. 2 shows an expanded view of the three specific areas denoted in fig. 1 by an encircled number.

The excitation source is a continuous-wave argon ion laser (CR-4, Coherent, Palo Alto, CA) giving 150 mW ultraviolet output (351–364 nm) and 9 W total visible output. Individual visible lines were obtained by use of a prism wavelength selector. For excitation at 325 nm, a helium-cadmium laser (Liconix, Sunnyvale, CA) is used. The beam is shuttered, attenuated by a variable reflective-type neutral density filter and filtered by a laser bandpass filter. The light is modulated by a double-crystal Pockels' cell driven by a multi-harmonic pulse generator with base frequency 4–7 MHz and usable harmonics to approx. 300 MHz. The multi-harmonic generation and detection equipment are components of a 48000 MHF fluorimeter (SLM Instruments, Urbana, IL) as described recently [2].

The reflected, modulated, and vertically polarized light from the Pockels' cell is reflected by a Q-switch prism, steered, and focused onto a 1 mm square front surfaced mirror for reflection onto the microscope objective and cell sample. The

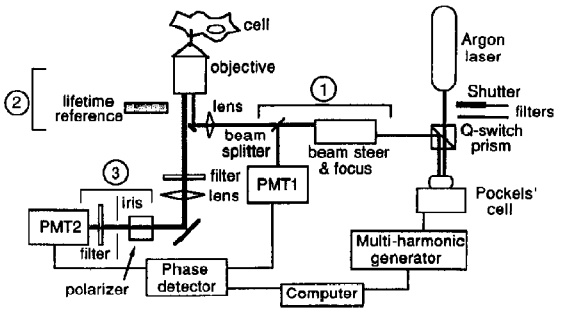

Fig. 1. Schematic diagram of the frequency-domain fluorescence microscope. See text for details.

beam steering device (component 1, fig. 2) consists of two front surfaced mirrors on gimbal mounts. The upper mirror has vertical adjustment. A thin quartz coverslip is mounted at 45° to reflect approx. 4% of the modulated beam onto PMT1 (R928 Hamamatsu) by a fiberoptic for timing/phase reference. A biconvex lens is mounted between the mirrors for beam focusing. The 1 mm front surfaced mirror was used instead of a dichroic mirror in most applications because of its high efficiency for reflection of the laser beam and transmission of emitted fluorescence. Importantly, wavelength-dependent emission depolarization by a dichroic mirror is eliminated when the emission path consists of air alone. The small mirror was immobilized on a 4 cm length of horizontal, 30 gauge steel tubing attached to a two-axis micropositioner which was secured to the microscope base. A lens was positioned 2 cm proximal to the small mirror to set the laser spot size in the focal plane without significant effect on the laser spot size on the 1 mm square mirror. Experiments could also be performed with a dichroic mirror provided that polarized intensities are corrected by an emission G factor or tensor [6].

The sample is positioned on the stage of a Nikon inverted epifluorescence microscope in which the internal optics are removed [7]. The objective is held in a threaded brass mount (component 2, fig. 2) with a 1.5 cm diameter cylindrical insert for introduction of a lifetime reference solid or solution in a sealed 10×10 or 10×2 mm cuvette. The cuvette is positioned at an angle of 10–20° from the horizontal to eliminate vertical beam reflection. The upper cuvette surface is blackened to eliminate light transmission to the cell sample. Emitted fluorescence is filtered by serial low-autofluorescence (KV series, Schott Glass) and high-efficiency cut-on filters. The light is collected by a fused silica lens for focus within the emission polarizer (see below) and reflected out of the microscope by a front surfaced mirror.

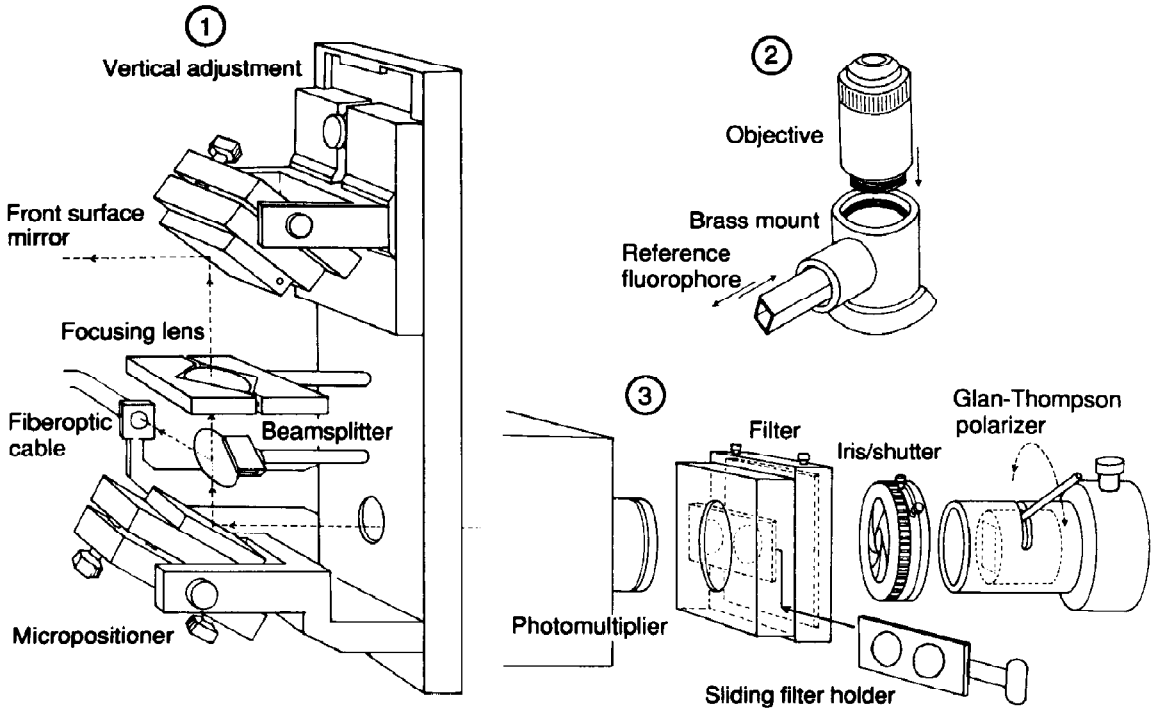

Fig. 2. Expanded schematic of beam steer and focus ①, objective and reference holder ② and emission optics ③. See text for details.

Importantly, the crown glass pentaprism used for eyepiece image viewing was replaced by a front surfaced mirror to avoid depolarization of emitted fluorescence. By external adjustment of the mirror, emitted light could be directed to the phase-sensitive photomultiplier or to an image analysis system (KS1380 microchannel intensifier and CCD camera, Videoscope, Washington, DC) for direct viewing.

Emitted fluorescence passed through a calcite Glan-Thompson polarizer positioned on a 90° rotatable mount. The light passed through a shutter, an adjustable circular iris, and optional neutral density and/or cut-on filters on sliding mounts (component 3, fig. 2). The introduction of a neutral density filter is particularly useful in some lifetime studies in which sample and reference solutions have remarkably different intensities. Sample fluorescence was detected by a selected R3896 photomultiplier (anode dark current 8.8 nA, cathode blue sensitivity 14 μA/lumen, Hamamatsu) which was dynode modulated to give multi-harmonic cross-correlation signals.

The microscope system has a usable wavelength range of 260–750 nm and has no depolarizing components. When the cell sample is replaced by a mirror and the emission cut-on filter is removed, there is a greater than 80-fold decrease in signal when the polarizer is rotated from vertical to horizontal orientation. Depolarization of emitted fluorescence by high numerical aperture (NA) objectives is an important concern as described below. Useful objectives with low autofluorescence and no strain-depolarization for fluorescence anisotropy decay measurements include 40 × quartz (glycerol immersion, NA 0.65, Leitz), 40 × and 100 × fluotar (oil immersion, variable NA 0.6–1.3, Nikon), 25 × long working distance (air, NA 0.25, Leitz) and 16 × quartz (air, NA 0.25, Leitz).

3.2. Data analysis

Analysis of lifetime and anisotropy decay is performed in the frequency domain by a comparative approach. For lifetime analysis, phase angles (ΔP) and modulation amplitudes (M_r) are determined from the difference and ratio, respectively, of absolute phase and modulation measured for sample and reference fluorophores; for anisotropy decay, ΔP and M_r are determined by comparison of parallel and perpendicular orientations of the emission polarizer [8].

Several modifications of previous analysis procedures have been made for biological applications. When steady-state background fluorescence is greater than 4% of sample fluorescence, sample ΔP and M_r are corrected by a modification of the principle described by Reinhart et al. [9]. Time-domain data for sample and background are phase adjusted by use of the reference PMT signal, subtracted, and converted to the frequency domain by inverse Fourier transform [10]. The correction procedure was effective even when background was greater than 75% of sample signal.

The selection of weighting factors and the calculation of χ^2 is particularly important for biological samples that have low signal intensity. Because data from the multi-harmonic acquisition are equally spaced in modulation frequency [2], data and fitted curves can be displayed on linear or logarithmic frequency axes. To minimize effects of large random fluctuations, ΔP and M_r at each frequency (ω) is determined from the median (rather than the mean) of four or more serial pairs of measurements. The standard deviation [sd(ω)] of each point, required for the weighted least-squares fitting procedure, is estimated either from the measured $sd_m(\omega)$ or by fitting $sd_m(\omega)$ to a smooth curve (generally two sets of third-order polynomials, one for $\omega < 150$ MHz and the other for $\omega > 150$ MHz). This method minimized the influence of abnormally high or low $sd_m(\omega)$ on the final fit. Model parameters for fitted lifetime or anisotropy decay functions, $Y_{fit}(\omega)$, were determined by least-squares minimization using an 80386 computer with 80387 math coprocessor [11],

$$\text{minimum} = \sum \left[Y_{fit}(\omega) - Y_{exp}(\omega) \right]^2 / sd(\omega)^2 \quad (1)$$

where $Y_{exp}(\omega)$ represents the experimental phase angles or modulation factors and the summation is taken over all phase angles and/or modulation factors. The steady-state anisotropy can be optionally included in the fit for anisotropy decay measurements.

A correction procedure was required to determine phase angles in lifetime microscopy studies in which the reference fluorophore was located in a different position from the sample fluorophore. The small time delay (t_d) imposed by the difference in pathlengths causes a frequency-dependent shift in phase angle by $d \cdot \omega / c$ where d denotes the difference in pathlength and c is the velocity of light. d was determined for each objective from the phase difference of an identical sample placed in the reference and sample positions.

4. Instrument performance

Fig. 3 (left) shows the dependence of phase angles and modulation factors on modulation frequency for an identical sample placed above the microscope stage and in the reference compartment. The longer light path resulted in a phase delay which was proportional to modulation frequency to approx. 250 MHz; the modulation amplitude remained near unity. It was confirmed using fluorescein samples (1–10 μM in 0.1 M NaOH) that the phase delay was independent of sample identity, but depended slightly upon objective because of the decreased velocity of light in solid media. These results validate the linearity of the multi-harmonic detection system and the phase correction procedure for lifetime determination.

Fig. 3 (right) shows the lifetime decay of BCECF measured by fluorescence microscopy. The average errors in phase angle and modulation were 0.1° and 0.01, respectively. The data fitted well to a single lifetime of 3.61 ns, not different from that measured by cuvette fluorimetry (3.60 ns).

The anisotropy decay of fluorescein was measured by phase-modulation microscopy and cuvette fluorimetry. Solutions consisted of 0.1 mM fluorescein and 0.1 N NaOH in 20% ethylene glycol/80% water and in 80% ethylene glycol/20% water (fig. 4, left). The viscosity of the latter solution was approx. 9 cP, causing a decrease in the fluorescein rotational rate. Measurements were made by 90° cuvette fluorimetry using a 10 × 10 mm cuvette and by epifluorescence microscopy, where solutions were sealed in 10 μl glass capillary tubes.

Differential phase angles and modulation factors were measured by comparison of data with emission polarizer parallel and perpendicular to the plane of excitation polarization. The data showed a remarkable difference in the phase angles and modulation factors for the two solutions; as predicted, the rotational correlation time for the more viscous sample (80% ethylene glycol) was approx. 10-times greater than that of the 20%

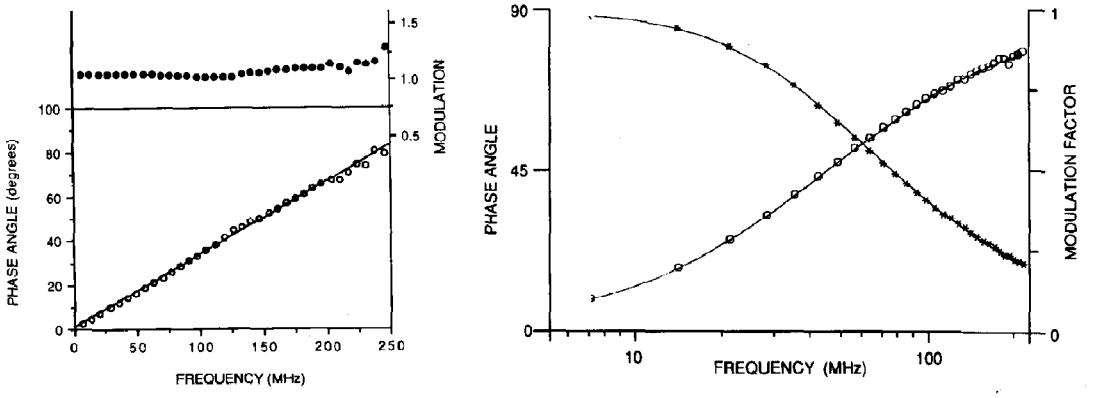

Fig. 3. Lifetime determination by phase-modulation microscopy. (Left) Phase angles and modulation values for reflected light. Light from the Ar laser (488 nm) was focused on a front-surfaced mirror in the sample and reference compartments. Reflected light was detected without filtration. (Right) Phase-modulation plot for lifetime decay of 10 μM BCECF in phosphate-buffered saline. The sample was placed in a 10 μl glass capillary tube and viewed with the 25× objective (NA 0.35). The reference was fluorescein in 0.1 N NaOH.

ethylene glycol sample (fig. 4, left). Importantly, there was little systematic difference between phase angles and modulation factors as measured by cuvette fluorimetry and epifluorescence microscopy.

Depolarization of emission fluorescence by high numerical aperture objectives has been proposed to be an important consideration in time-resolved polarization microscopy [6,12–14]. Depolarization is predicted because of the ability of the objective to 'see around' the fluorophore so that components of fluorescence emission along the optical axis are detected. The effect depends upon objective numerical aperture, refractive index, the geometric distribution of fluorophores and the time-resolved fluorophore rotation [12,13]. Because of the theoretical complexity and uncertain parameters required to make a rigorous correction, we have evaluated objective depolarization by comparing results obtained by several objectives of differing numerical apertures as shown in fig. 4 (right). The sample consisted of 0.1 mM fluorescein and 0.1 M NaOH in 70% glycerol/30% water; a viscous solution (~ 30 cP) was chosen because objective depolarization effects should be largest with slowly rotating or hindered fluorophores. The results show very little systematic deviation of differential phase angles and modulation amplitudes on objective numerical aperture in the range from approx. 0.05 (cuvette) to 1.3 (40 × oil objective). Therefore, it is unlikely that objective depolarization effects are significant in the samples examined here.

The frequency-domain microscope was used to measure lifetime and anisotropy of a fluid-phase fluorophore in a subcellular domain. Fig. 5 shows a single Swiss 3T3 fibroblast labeled with the fluorophore 6CF. Fluorescence was excited in a smaller than 1 μm circular area in peripheral cytoplasm as indicated by the focused laser spot

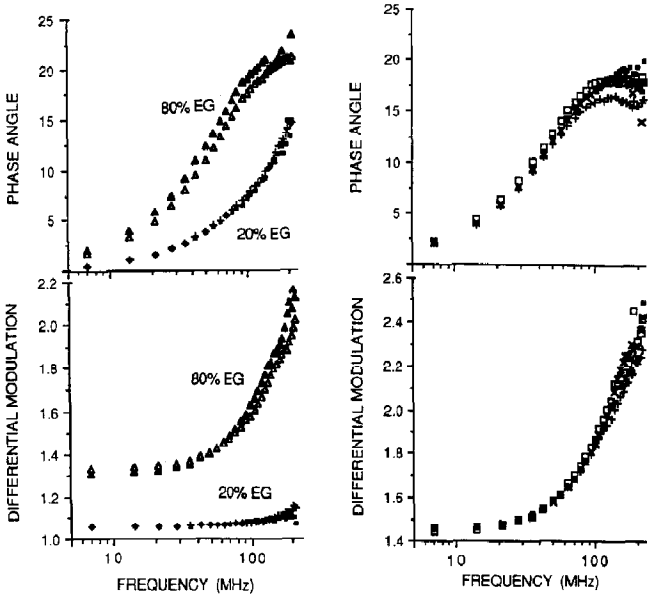

Fig. 4. Anisotropy decay determination by phase-modulation microscopy. (Left) Anisotropy decay of 0.1 mM fluorescein and 0.1 M NaOH in 80% ethylene glycol/20% water and 20% ethylene glycol/80% water. Measurements were made by cuvette fluorimetry and fluorescence microscopy using the 40× quartz objective (glycerol immersion, NA 0.65). (◆, ▲) Cuvette; (+, △) microscope. Fitted rotational correlation times were 1.2 ns (80% ethylene glycol) and 140 ps (20% ethylene glycol). (Right) Anisotropy decay of 0.1 mM fluorescein and 0.1 M NaOH in 70% glycerol/30% water measured in a cuvette (■) and by microscopy using the 25× objective (air, NA 0.35, +), 40× objective (oil, NA 0.60, ×) and 40× objective (oil, NA 1.30, □).

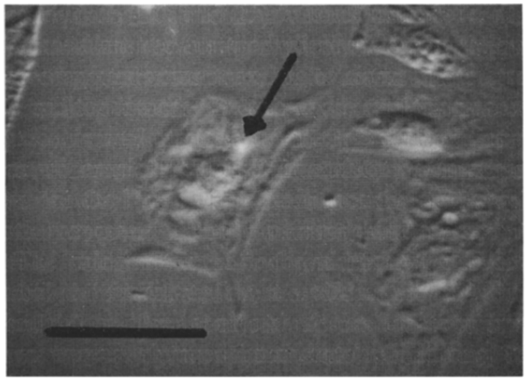

Fig. 5. Fluorescence micrograph of a 6CF-labeled Swiss 3T3 fibroblast viewed with Hoffman optics and illuminated with a focused 488 nm laser spot (arrow) in the frequency-domain microscope. Scale bar: 10 μm.

(see arrow). The diameter of the laser spot was determined by the focal length of the lens proximal to the mirror in fig. 1.

Fig. 6 (left) shows a phase-modulation plot for the fluorescence decay of 6CF using the focused laser spot. To minimize photobleaching and photodynamic cell injury, the full measurement was made in less than 30 s of cell illumination time. There was less than 10% photobleaching in a 30 s exposure. Adequate data (to ~ 0.25 ns accuracy in lifetime determination) was obtained with 1 s of cell illumination time. To eliminate polarization artifact, an emission polarizer was positioned at 54.7° (the 'magic angle' [15]) from the 'parallel' orientation, where parallel is defined by the polarization axis of reflected excitation light. An alternative approach would be to use a polarization randomizer in the excitation path distal to the Q-switch prism. Typical errors for phase and modulation measurements are shown as standard deviations. Repeat determinations of lifetimes in different cells or in several regions of a single cell were reproducible to within 0.2 ns. The plot was not different when the focal plane of the objective was changed to illuminate a 5 μm area.

Fig. 6 (right) shows the anisotropy decay of 6CF in fibroblasts. Differential phase angles and modulation amplitudes were measured from pairs of data acquired at parallel and perpendicular orientations of the emission polarizer. The cell was viewed with the 40 × quartz objective (NA 0.65). The data were fitted to a rotational model for anisotropic decay [8,11] with two rotational correlation times of 180 ps and 23.1 ns ($\chi^2 = 1.09$); the fractional intensity corresponding to the faster rotation was 0.57. To show that significant depolarization by the microscope objective did not occur in this system, similar parameters were obtained by use of a 25 × objective (NA 0.35). The correlation time of the faster rotation has been taken to be a measure of the cytoplasmic viscosity of the fluid-phase in the 'open' region away from

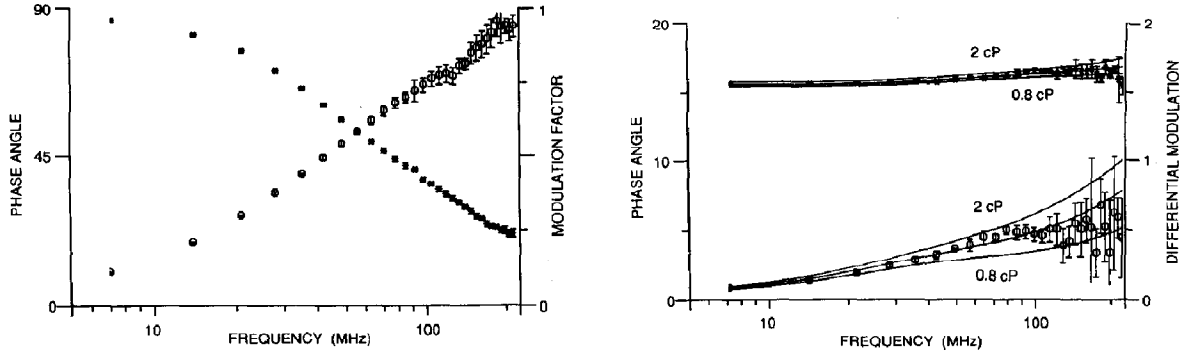

Fig. 6. Lifetime (left) and anisotropy decay (right) of 6CF in cytoplasm of a Swiss 3T3 fibroblast. Lifetime reference was fluorescein in 0.1 N NaOH (4.6 ns). Fitted lifetime was 3.88 ns. Anisotropy decay was fitted to a two-component anisotropy decay model with correlation times of 180 ps and 23.1 ns; the fractional component corresponding to the shorter correlation times was 0.57. The shorter correlation time corresponds to a cytoplasmic viscosity of 1.3 cP (see text). Comparison curves for viscosities of 0.8 and 2 cP are shown.

cytoskeletal elements [16]. The fitted data give a viscosity of 1.3 cP. Differential phase angle and modulation amplitudes predicted for viscosities of 0.8 and 2 cP are shown for comparison to evaluate the sensitivity of the fit.

5. Discussion

The goals of this study were to develop the specialized optics and analysis procedures to make frequency-domain measurements of fluorescence lifetime and anisotropy decay in submicron regions of living cells. The parallel acquisition capabilities of the multi-harmonic cross-correlation method make feasible the resolution of complex picosecond decay kinetics rapidly in labile and photosensitive biological samples including living cells and epithelial tissues. Lifetimes were measured without moving the sample by use of a reference fluorophore positioned proximal to the microscope objective. Anisotropy decay was measured by use of a rotatable polarizer in the emission path as described recently for the quantitative imaging of steady-state anisotropy [6,7]. Microscope optics were selected to minimize instrument depolarization of excitation and emission light and to maximize collected fluorescence. The data showed excellent agreement between lifetimes and anisotropy decay measured by cuvette fluorimetry and fluorescence microscopy, and demonstrated the ability to measure lifetime and anisotropy decay in subcellular domains.

There are many unexplored applications of frequency-domain microfluorimetry in cell biology. Measurement of the picosecond correlation time for rotation of fluid-phase fluorophores provides direct information about cytoplasmic viscosity [16] which complements previous studies of dye migration, photobleaching recovery and ESR [17,18]. Measurement of the rotational characteristics of fluorophores in lipid membranes or bound to membrane proteins provides information about membrane dynamics [19]. Because experiments are performed in living cells, the influence of hormonal effectors on cytoplasmic and membrane dynamics can be evaluated in real time. Lifetime heterogeneity analysis of fluorophores should be of application in the identification of microcompartmentation in cell cytoplasm and domain formation in cell membranes [20,21]. The measurement of lifetimes of ion-sensitive intracellular fluorophores such as indo-1 and SPQ may provide absolute values for cell ion activity which do not depend upon dye density or inner filter effects [22]. Similarly, lifetime determination would provide the least ambiguous values of energy-transfer efficiency in studies of vesicle fusion and donor–acceptor distance. Finally, the use of time-resolved microfluorimetry methods is important in microanalytical studies of bulk solutions when little sample is available, and for very dim samples which require the highly efficient collection of fluorescence.

There are a number of concerns and limitations in the measurement of time-resolved microfluorescence by frequency-domain methods. The minimal spatial resolution is approx. 0.5 μm with a 100 $\times$ objective in wide-field microscopy as determined by the Airy function [23], however, improved resolution is possible by confocal optics or by positioning a pinhole in the detection optics. As in scanning confocal microscopy, there may be considerable photobleaching and photodynamic cell injury by use of a focused laser spot in the image focal plane. In lifetime measurements, accurate values of reference/sample delay time must be obtained to prevent artifact in multi-component analysis. In anisotropy decay measurements, polarizer alignment and the use of calibration standards are necessary in every set of measurements. Possible objective depolarization should be evaluated empirically by comparison of data obtained with objectives of differing numerical aperture. In biological samples having dim fluorescence or requiring excitation below 400 nm, background (sample minus fluorophore) fluorescence must be subtracted in every measurement. If background fluorescence is more than 10% of sample fluorescence, it is important to measure a true background signal before cell labeling, or if possible, by destaining cells at the completion of the experiment.

Bearing these difficulties in mind, time-resolved microfluorimetry measurements are feasible in selected regions of single cells and should have

novel applications in studies of dynamics in living cells [24].

Acknowledgments

This work was supported by grants DK39354, DK35124 and DK16095 from the National Institutes of Health and a grant from the National Cystic Fibrosis Foundation. We thank Kerry Swift and George Mitchell for continuing advice and technical support. K.F. is a fellow of the National Kidney Foundation. A.S.V. is an established investigator of the American Heart Association.

References

1 E. Gratton, B. Feddersen and M. van de Ven, in: Proceedings of the International Society for Optical Engineering, ed. J.R. Lakowicz (1990) vol. 1204, p. 21.
2 G.W. Mitchell and K. Swift, in: Proceedings of the International Society for Optical Engineering, ed. J.R. Lakowicz (1990) vol. 1204, p. 270.
3 D.J. Birch, K. Suhling, A.S. Holmes, A.D. Dutch and R.E. Imhof, in: Proceedings of the International Society for Optical Engineering, ed. J.R. Lakowicz (1990) vol. 1204, p. 26.
4 Suzuki, Y. Tsuchiya, K. Kinoshita, M. Sugiyama and E. Inuzuka, Phil. Trans. R. Soc. Lond. A298 (1980) 295.
5 A.C. Chao, J.A. Dix, M. Sellers and A.S. Verkman, Biophys. J. 56 (1989) 1071.
6 K. Fushimi, J.A. Dix and A.S. Verkman, Biophys. J. 57 (1990) 241.
7 J.A. Dix and A.S. Verkman, Biophys. J. 57 (1990) 231.
8 J.R. Lakowicz, Principles of fluorescence spectroscopy (Academic Press, New York, 1983) p. 112.
9 G.D. Reinhart, B. Feddersen, D.M. Jameson and E. Gratton, Biophys. J. 57 (1990) 189a (Abstr.).
10 K. Swift, G. Mitchell, M. Armijo and A.S. Verkman, Biophys. J. (1991) in the press (Abstr.).
11 T. Calafut, J.A. Dix and A.S. Verkman, Biochemistry 28 (1989) 5051–5058.
12 D. Axelrod, Biophys. J. 26 (1979) 557.
13 D. Axelrod, Methods Cell Biol. 30 (1989) 333.
14 K. Florine-Casteel, Biophys. J. 57 (1990) 1199.
15 G. Weber, Biochem. J. 51 (1952) 155.
16 K. Fushimi and A.S. Verkman, J. Cell Biol. 112 (1991) in press.
17 K. Luby-Phelps, D.L. Taylor and F. Lanni, J. Cell Biol. 102 (1986) 2105.
18 K.R. Porter, J. Cell Biol. 99 (1984) 3s.
19 F. Mulders, H. van Langen, G. van Ginkel and Y.K. Levine, Biochim. Biophys. Acta 859 (1986) 209.
20 R.D. Klausner and A.M. Kleinfeld, in: Cell surface dynamics, eds. A.S. Perelson, C. Delisis and F.W. Wiegel (Dekker, New York, 1984) p. 23.
21 D.M. Haverstick and M. Glaser, J. Cell Biol. 106 (1988) 1885.
22 A.S. Verkman, Am. J. Physiol. 259 (1990) C375.
23 S. Inoue, Methods Cell Biol. 30 (1989) 85.
24 A.S. Verkman, Commun. Cell. Mol. Biophys. (1991) in press.